Evolution of infrared photoreflectance lineshape with temperature in narrow-gap HgCdTe epilayers

Jun Shao,[1,a)] Lili Ma,[1] Xiang Lü,[1] Wei Lu,[1] Jun Wu,[2] F.-X. Zha,[3] Y.-F. Wei,[2] Z.-F. Li,[1] S.-L. Guo,[1] J.-R. Yang,[2] Li He,[2] and J.-H. Chu[1,4]
[1]*National Laboratory for Infrared Physics, Shanghai Institute of Technical Physics, Chinese Academy of Sciences, 200083 Shanghai, People's Republic of China*
[2]*Research Center for Advanced Materials and Devices, Shanghai Institute of Technical Physics, Chinese Academy of Sciences, 200083 Shanghai, People's Republic of China*
[3]*Physics Department, Shanghai University, 200444 Shanghai, People's Republic of China*
[4]*Key Laboratory of Polar materials and Devices, Ministry of Education, East China Normal University, 200062 Shanghai, People's Republic of China*

(Received 4 August 2008; accepted 16 September 2008; published online 2 October 2008)

Temperature-dependent (11–290 K) infrared photoreflectance (PR) measurements are performed on as-grown arsenic-doped HgCdTe epilayers in a midinfrared spectral region. Main PR features near bandedge manifest clear evolution of lineshape with temperature, of which the fittings identify besides a band-band process several below-gap processes. Analyses show that these features are due to photomodulation-induced screening of donor-acceptor pairs and photomodulation of band-impurity and band-band reflectance, their intensities correlate to the joint concentration of the involved energetic states. Temperature-dependent infrared PR may be a right optical spectroscopy for identifying impurity levels in semiconductors such as HgCdTe with high-density impurities.
 [DOI: 10.1063/1.2996030]

Photoreflectance (PR) is a modulation spectroscopy having been employed widely in characterizing semiconductor electronic band structures.[1] Its derivative nature suppresses uninteresting background and emphasizes structures located at the energy range of interband transitions and other weak features. After the observation of below-gap PR feature in bulk GaAs,[2] efforts have been made for clarifying its mechanism.[3–6] While some of the studies concluded the below-gap feature to be linked to impurity absorption,[2,3] others suggested either a pure back-surface reflection (BSR) effect[4] or a joint effect of BSR and impurity absorption.[5] Furthermore, as the PR measurements were carried out only under some particular temperatures, possible competition between the below-gap and band-gap PR features was not observed, and the evolution with temperature was not clarified.

HgCdTe as a distinct narrow-gap semiconductor has attracted wide range of research interests. It is the material system of choice for high performance infrared detector arrays, while it can serve as a good example for fundamental physics study.[7,8] The nature of high density of shallow-level defects/impurities warrants it a good candidate for clarifying the mechanism of below-gap PR features. Unfortunately, such PR features fall usually into a mid- or even far-infrared spectral region, which is generally beyond the power of a conventional PR technique.[9]

In this work, PR study of as-grown arsenic-doped $Hg_{0.713}Cd_{0.287}Te$ epilayers is carried out using a Fourier-transform infrared spectrometer-based PR technique.[9] The advantages of high signal-to-noise ratio and low experimental time cost of the technique[10,11] ensure a reliable measurement in a temperature range of 11–290 K. The sample was grown in a Riber 32P molecular-beam epitaxy system on an undoped semi-insulating GaAs (211)B substrate at a temperature of around 183 °C.[12] A pure arsenic source was used for doping, and the dopant concentration was about 6×10^{18} cm^{-3}. The sample is *p*-type at 77 K with a carrier density of 9.35×10^{15} cm^{-3} due to high density of mercury vacancies.[13] It is *n*-type at room temperature because arsenic atoms reside predominantly at the cation side and are thermally excited at high temperature.[14,15] Curve fittings of PR spectra are performed with a lineshape function for low electrical field modulation,[1] and the "intensity" of PR feature is evaluated with the cosine term set to unity.[16] For comparison, photoluminescence (PL) spectra are recorded by modulated PL technique,[17] and simple curve-fitting procedure is performed[18] to identify the transitions around band gap.

Figure 1 depicts infrared PR spectra for the HgCdTe sample at different temperatures. The evolution of individual PR features with temperature is traced out by dash-dots and marked with D1, D2, DA, B1, B2, and B3, respectively. For clarity, the positive extrema are taken for each of the features. Obviously, the main PR features, which are the major interest of this study, are contributed in turn by B1, B2, and B3 as temperature rises. Therefore, they cannot be attributed solely to band-band but may be dominated by either interband or below-band processes at a particular temperature. The movement of the main PR features with temperature to higher energy is similar to the band-gap behavior. This is analogous to the study of Röpplscher *et al.* of GaAs.[4] Note, however, that there only a very weak steplike below-gap PR feature was observed, which was attributed to BSR-induced electromodulation of the field broadened excitonic absorption tail. For a narrow-gap HgCdTe, even if there were excitonic effects, the exciton binding energy is, as expected, less than 1 meV.[19] Moreover, a comparison of PR and PL spectra for HgCdTe samples with different arsenic doping levels indicates that each of the main PR features has in corresponding PL spectrum a counterpart at similar energy. The BSR effect as mechanisms of below-band PR processes can hence be safely excluded. For the low-energy D1 and D2 features, the enhancement in intensity with temperature seems to be

[a)]Author to whom correspondence should be addressed. Electronic mail: jshao@mail.sitp.ac.cn.

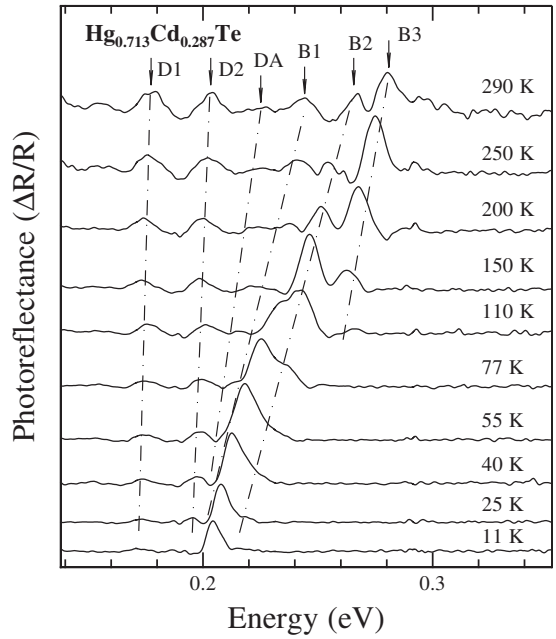

FIG. 1. PR spectra for HgCdTe sample in identical intensity scale but different offsets. Dash-dots track features' evolution.

similar to the study of GaAsN and GaInAsN, which was ascribed to the effect of carrier localization at bandedge.[20] Nevertheless, BSR-induced interference may also be a possible reason.[21]

To get a closer view of the lineshape evolution, curve fittings of the PR spectra are plotted in Fig. 2 for several representative temperatures. The critical-point positions are marked by arrows and labels. For comparison, PL spectra taken at nominally identical temperatures are also plotted together with fitting curves. As illustrated in Fig. 2(a), only B1 and B2 features are identifiable from the main PR signal at 11 K and B2 is rather weak relative to B1. Meanwhile, the PL spectrum can be fitted by a superposition of two components, of which the energetic positions are, respectively, very close to those of B1 and B2 PR features. The case is similar at 40 K, as shown in Fig. 2(b). This situation changes at higher temperature. As depicted in Fig. 2(c), three PR features of B1, B2, and B3 are clearly identified at 110 K, and B2 dominates though B1 is still strong and B3 emerges. Besides, another weak feature, DA, can be identified at the left side of B1. Correspondingly, the PL spectrum can be well reproduced by three components with comparable intensities, and the two lower-energy ones are energetically close to the critical-point positions of B1 and B2. At 150 K, B1 losses most of its intensity, as indicated in Fig. 2(d), while B3 gets stronger. The PL spectrum, on the other hand, can be well fitted only when four transitions are assumed, of which three lower-energy transitions are energetically close to B1, B2, and B3 features.

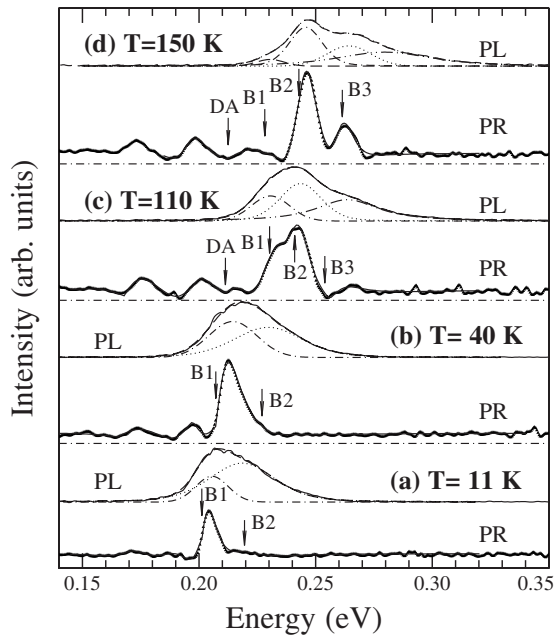

FIG. 2. PR and PL spectra for $Hg_{0.713}Cd_{0.287}Te$ sample at (a) 11 K, (b) 40 K, (c) 110 K, and (d) 150 K, overlaid by fitting curves. Arrows and labels mark PR critical points.

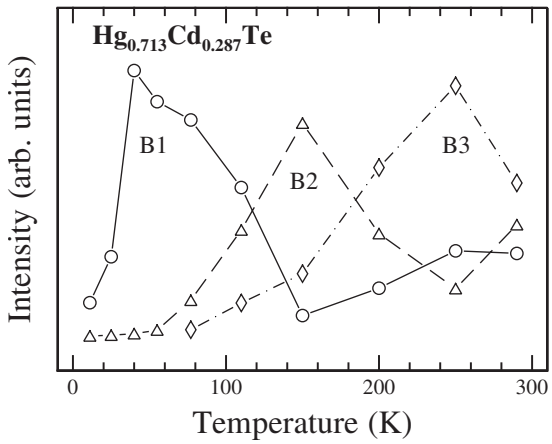

FIG. 3. Intensity vs temperature in open circles, triangles, and diamonds for B1, B2, and B3 PR features, respectively. Lines connect the individual sets of points to guide the eyes.

As general remarks (i) the energy separation between B1 and B3 is about 32 meV, while that between B1 and B2 is about 14 meV at low temperature and 18 meV at high temperature. (ii) The main PR features move to higher energy with temperature, the low-energy D1 and D2 features, however, do not show obvious change in energy and lineshape but clear enhancement in intensity. (iii) The PL peak occurs in the energy range where the main PR features show up, and each of the PL fitting components corresponds energetically to a particular main PR features. (iv) The PL spectrum does not manifest detectable signal in the energy range where low-energy D1, D2, and DA PR features occur. According to a previous study,[22] the PL spectra of a $Hg_{0.68}Cd_{0.32}Te$ sample with impurity density of 10^{15} cm^{-3} are contributed by band-band, band-acceptor and donor-acceptor transitions at 4.6–30 K. The band-band transition is less intense at low temperature but becomes predominant and band-filling effect shows up at high temperature. As a result, a shoulder may emerge on the higher energy side of the PL peak. It is hence inferable that the main PR features are likely irrelevant to band-filling effects in the temperature range considered.

Figure 3 plots the main PR features' intensities against temperature. B1 dominates the main PR signal and experiences an enhancement in the temperature range of 11–40 K. As temperature rises further, B1 dies away while B2 becomes stronger until about 150 K. Then B2 begins to diminish, and B3 gains its strength and becomes the major contributor when the temperature exceeds about 200 K.

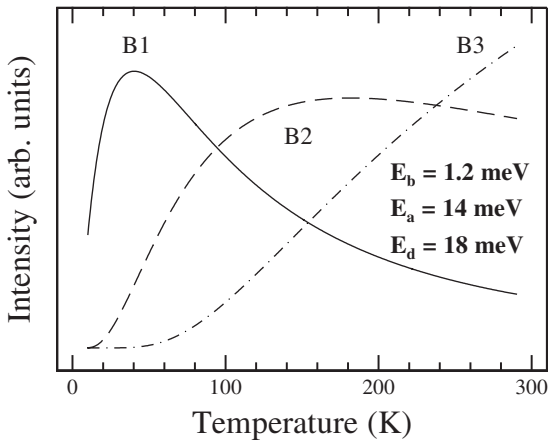

FIG. 4. Simulation of the intensity vs temperature for B1, B2, and B3 PR features, respectively.

By taking the observation into account and keeping the textbook knowledge in mind that a shallow impurity will be thermally activated at high temperature, it can be inferred that (i) there should be one donor and one acceptor levels involved in the main PR features, and (ii) while B1 may be linked to weakly bounded donor-acceptor pairs, B2 may be related to acceptor-conduction band and valence band-donor processes and B3 to the joint concentration of free electrons and holes. The intensities of B1, B2, and B3 can hence be estimated by assuming that the equilibrium concentration of holes (majority carrier at low temperature) from acceptors follows $e^{-E_a/2k_BT}$ relation, while electrons (minority carrier at low temperature) from thermal ionization of donors follow the standard calculation of statistical mechanics of hydrogen atoms,[23]

$$I_1(T) \propto e^{-E_b/k_BT}(1-e^{-E_d/k_BT})(1-e^{-E_a/2k_BT}),$$

$$I_2(T) \propto e^{-E_d/k_BT}(1-e^{-E_a/2k_BT}) + (1-e^{-E_d/k_BT})e^{-E_a/2k_BT},$$

$$I_3(T) \propto e^{-E_d/k_BT}e^{-E_a/2k_BT}, \quad (1)$$

where T and k_B are temperature and Boltzmann constant, E_b denotes the binding energy of donor-acceptor pair, and E_d and E_a represent the thermal ionization energies of donor and acceptor, respectively.

The intensities of the main PR features are calculated with assumption of E_b=1.2 meV, E_a=14 meV, and E_d =18 meV; the results are plotted in Fig. 4. The simulation mimics the enhancement of B1 and B2 with temperature quite well, with the maxima showing at similar temperatures as manifested by experimental data. The slow decay of B2 and monotonic increase in B3 at high temperature may be due to the fact that the calculation does not consider the effects of phonon scattering and screening of free electrons, which will cause a reduction in PR modulation efficiency at high temperature.

These results indicate that the main PR features are not a BSR effect but related to shallow impurities. The intensities correlate to the joint concentration of related lower and upper states and are dominated by different processes at different temperatures. B1 feature originates from photomodulation-induced screening of donor-acceptor pairs, similar to the screening of bound-state exciton.[24] B2 is due to photomodulation of built-in electric field, which causes acceptor-conduction band and valence band-donor reflectance to be modulated, similar to the B3 band-band process.[25] In neither case can the main PR features be related to impurity absorption processes. This is in clear contrast to the previous below-gap PR study[2,3,5] but is consistent with the knowledge that in bulk semiconductors the contribution of the absorptive component to band-band PR process is negligible.[26] The related donor and acceptor levels locate at ~18 meV below the conduction band and ~14 meV above the valence band. Donors and acceptors form pairs at extremely low temperature with a binding energy of ~1.2 meV. Temperature-dependent PR is promisingly a right choice of optical spectroscopy for investigating impurity levels and bandedge electronic structures in semiconductors with relatively high density of impurities.

This work was sponsored by Program of Shanghai Subject Chief Scientist (No. 08XD14047), STCSM (No. 06JC14072), NSFC (Nos. 60676063 and 60406011), SKPBR (No. 2007CB924901), and Knowledge Innovation Program of CAS, China.

[1] F. H. Pollak and H. Shen, Mater. Sci. Eng., R. **10**, 275 (1993).
[2] O. J. Glembocki, N. Bottka, and J. E. Furneaux, J. Appl. Phys. **57**, 432 (1985).
[3] X. Yin, F. H. Pollak, L. Pawlowicz, T. O'Neill, and M. Hafizi, Appl. Phys. Lett. **56**, 1278 (1990).
[4] H. Röppischer, N. Stein, U. Behn, and A. B. Novikov, J. Appl. Phys. **76**, 4340 (1994).
[5] R. Tober and J. D. Bruno, J. Appl. Phys. **68**, 6388 (1990).
[6] P. W. Yu, J. D. Clark, D. C. Look, C. Q. Chen, J. Yang, E. Koutstis, M. A. Khan, D. V. Tsvertkov, and V. A. Dmitriev, Appl. Phys. Lett. **85**, 1931 (2004).
[7] B. Gelmont, K.-S. Kim, and M. Shur, Phys. Rev. Lett. **69**, 1280 (1992).
[8] F. Fuchs, H. Schneider, P. Koidl, K. Schwarz, H. Walcher, and R. Triboulet, Phys. Rev. Lett. **67**, 1310 (1991).
[9] J. Shao, F. Yue, X. Lü, W. Lu, W. Huang, Z. Li, S. Guo, and J. Chu, Appl. Phys. Lett. **89**, 182121 (2006).
[10] J. Shao, W. Lu, F. Yue, X. Lü, W. Huang, Z. Li, S. Guo, and J. Chu, Rev. Sci. Instrum. **78**, 013111 (2007).
[11] J. Shao, W. Lu, M. Sadeghi, X. Lü, S. M. Wang, L. Ma, and A. Larsson, Appl. Phys. Lett. **93**, 031904 (2008).
[12] L. He, J. R. Yang, S. L. Wang, S. P. Guo, M. F. Yu, X. Q. Chen, W. Z. Fang, Y. M. Qiao, Q. Y. Zhang, R. J. Ding, and T. L. Xin, J. Cryst. Growth **175/176**, 677 (1997).
[13] Y. S. Ryu, Y. B. Heo, B. S. Song, S. J. Yoon, Y. J. Kim, and T. W. Kang, Appl. Phys. Lett. **83**, 3776 (2003).
[14] F. Aqariden, H. D. Shih, M. A. Kinch, and H. F. Schaake, Appl. Phys. Lett. **78**, 3481 (2001).
[15] Y. Selamet, C. H. Grein, T. S. Lee, and S. Sivananthan, J. Vac. Sci. Technol. B **19**, 1488 (2001).
[16] T. J. C. Hosea, D. Lancefield, and N. S. Garawal, J. Appl. Phys. **79**, 4338 (1996).
[17] J. Shao, W. Lu, X. Lü, F. Yue, Z. Li, S. Guo, and J. Chu, Rev. Sci. Instrum. **77**, 063104 (2006).
[18] J. Shao, R. Winterhoff, A. Dörnen, E. Baars, and J. Chu, Phys. Rev. B **68**, 165327 (2003).
[19] J. W. Tomm, K. H. Herrmann, and A. E. Yunovich, Phys. Status Solidi A **122**, 11 (1990).
[20] R. Kudrawiec, G. Sęk, J. Misiewicz, L. H. Li, and J. C. Harmand, Appl. Phys. Lett. **83**, 1379 (2003).
[21] D. Huang, D. Mui, and H. Morkoç, J. Appl. Phys. **66**, 358 (1989).
[22] A. T. Hunter, D. L. Smith, and T. C. McGill, Appl. Phys. Lett. **37**, 200 (1980).
[23] C. Kittel, *Introduction to Solid State Physics*, 8th ed. (Wiley, Hoboken, 2005).
[24] W. A. Albers, Phys. Rev. Lett. **23**, 410 (1969).
[25] R. E. Wagner and A. Mandelis, Phys. Rev. B **50**, 14228 (1994).
[26] B. V. Shanabrook, O. J. Glembocki, and W. T. Beard, Phys. Rev. B **35**, 2540 (1987).